2012

Efficient ^{18}F-Labeling of Large 37-Amino-Acid pHLIP Peptide Analogues and Their Biological Evaluation

Pierre Daumar

Cindy A. Wanger-Baumann

See next page for additional authors

Citation/Publisher Attribution

Daumar, P., Wanger-Baumann, C. A., Pillarsetty, N., Fabrizio, L., Carlin, S. D., Andreev, O. A., Reshetnyak, Y. K., & Lewis, J. S. (2012). Efficient ^{18}F-Labeling of Large 37-Amino-Acid pHLIP Peptide Analogues and Their Biological Evaluation. *Bioconjugate Chem.*, *23*(8), 1557-1566. doi: 10.1021/bc3000222
Available at: https://doi.org/10.1021/bc3000222

Published in final edited form as:
Bioconjug Chem. 2012 August 15; 23(8): 1557–1566. doi:10.1021/bc3000222.

Efficient ^{18}F-Labeling of Large 37-Amino Acid pHLIP Peptide Analogues and their Biological Evaluation

Pierre Daumar[1,§], **Cindy A. Wanger-Baumann**[1,§], **NagaVaraKishore Pillarsetty**[1], **Laura Fabrizio**[1], **Sean D. Carlin**[1], **Oleg A. Andreev**[3], **Yana K. Reshetnyak**[3], and **Jason S. Lewis**[1,2]

[1]Department of Radiology, Memorial Sloan-Kettering Cancer Center, New York, NY 10065, USA

[2]Program in Molecular Pharmacology and Chemistry, Memorial Sloan-Kettering Cancer Center, New York, NY 10065, USA

[3]Physics Department, University of Rhode Island, Kingston, RI 02881

Abstract

Solid tumors often develop an acidic microenvironment, which plays a critical role in tumor progression and is associated with increased level of invasion and metastasis. The 37-residue pH (low) insertion peptide (pHLIP®) is under study as an imaging platform because of its unique ability to insert into cell membranes at a low extracellular pH (pH_e<7). Labeling of peptides with [^{18}F]-fluorine is usually performed via prosthetic groups using chemoselective coupling reactions. One of the most successful procedures involves the alkyne-azide copper(I) catalyzed cycloaddition (CuAAC). However, none of the known “click” methods have been applied to peptides as large as pHLIP. We designed a novel prosthetic group and extended the use of the CuAAC “click chemistry” for the simple and efficient ^{18}F-labeling of large peptides. For the evaluation of this labeling approach, a D-amino acid analogue of WT-pHLIP and a L-amino acid control peptide K-pHLIP, both functionalized at the N-terminus with 6-azidohexanoic acid, were used. The novel 6-[^{18}F]fluoro-2-ethynylpyridine prosthetic group, was obtained via nucleophilic substitution on the corresponding bromo-precursor after 10 min at 130 °C with a radiochemical yield of 27.5 ± 6.6% (decay corrected) with high radiochemical purity ≥ 98%. The subsequent Cu^{I} catalyzed “click” reaction with the azido functionalized pHLIP peptides was quantitative within 5 min at 70 °C in a mixture of water and ethanol using Cu-acetate and sodium L-ascorbate. [^{18}F]-D-WT-pHLIP and [^{18}F]-L-K-pHLIP were obtained with total radiochemical yields of 5–20% after HPLC purification. The total reaction time was only 85 min including formulation. *In vitro* stability tests revealed high stability of the [^{18}F]-D-WT-pHLIP in human and mouse plasma after 120 min, with the parent tracer remaining intact at 65 and 85%, respectively. PET imaging and biodistribution studies in LNCaP and PC-3 xenografted mice with the [^{18}F]-D-WT-pHLIP and the negative control [^{18}F]-L-K-pHLIP revealed pH-dependent tumor retention. This reliable and efficient protocol promises to be useful for the ^{18}F-labeling of large peptides such as pHLIP and will accelerate the evaluation of numerous [^{18}F]-pHLIP analogues as potential PET tracers.

Keywords

Fluorine-18; tumor microenvironment; peptides; pH

Corresponding Author: Jason S. Lewis, Ph.D., Radiochemistry Service, Department of Radiology, Memorial Sloan-Kettering Cancer Center, 1275 York Avenue, New York, NY10065, Tel: 1-646-888-3038, Fax: 1-646-422-0408, lewisj2@mskcc.org.
[§]These authors contributed equally to this work.

Disclosures: No disclosure.

INTRODUCTION

Positron Emission Tomography (PET) is a non-invasive functional *in vivo* imaging modality, commonly used in tumor diagnosis. Tremendous effort has been made towards the development of additional efficient and widely applicable PET tracers, given the limitations of [^{18}F]-FDG, for the targeting of a large variety of cancers. However, the development of a universal tumor targeting PET tracer is limited due to tumor heterogeneity and differences within the tumor environment.[1] Therefore, targeting a physiological anomaly present in most cancers seems very promising for the development of a widely applicable diagnostic agent in oncology. The acidity of the tumor microenvironment is one of such anomalies, which plays a significant role in progression and is often associated with increased invasion and metastasis.[2] It is present in 90% of tumor microenvironments and is therefore considered a promising environmental marker for targeting.[3, 4]

A 37-residue peptide discovered in 1997 by Hunt *et al.*[5] was recently shown to display unique pH-dependent properties: the pH Low Insertion Peptide (WT-pHLIP, NH_2-ACEQNPIYWARYADWLFTTPLLLLDLALLVDADEGTG-CO_2H) is soluble in aqueous solution at physiological pH and shows transient interaction with cell membranes in tissues with neutral extracellular pH (pH_e). In tissues with an acidic pH_e, Asp/Glu residues of pHLIP are protonated, which increases the overall hydrophobicity of the peptide and affinity to the cell membrane. As a result, pHLIP inserts and translocates itself through the phospholipid bilayer that is the cellular membrane.[6] This insertion involves a change in the peptide conformation to a α-helix, the *N*-terminus remaining in the extracellular space, while the C-terminus reaches the intracellular lumen.

The pHLIP peptide was recognized as a potentially useful platform for tissue acidity imaging and therefore, its potential application as a universal tool in oncology was envisaged.[7] We successfully demonstrated that fluorescent pHLIP could be used to detect tissue acidity and target tumors in mice.[8] In an extension to the study, ^{64}Cu-labeled pHLIP was evaluated for its suitability as a PET tumor imaging agent. The novel tracer displayed good imaging characteristics with the highest level of radioactivity accumulation in LNCaP tumor being reached 1 h after administration, but some demetallation[9] and a significant retention of activity in the GI tract were also observed.

Fluorine-18 is the most common PET nuclide due to its favorable physical properties (low positron energy, pure positron decay and 110 min half-life), availability, and dosimetry.[10, 11] Therefore, the ^{18}F-nuclide was considered the ideal non-metal based alternative for the PET-labeling of pHLIP and its analogues. However, the ^{18}F-labeling of large peptides such as WT-pHLIP (molecular weight (MW) > 4000 Da) still remains challenging because nucleophilic substitution with [^{18}F]-fluoride requires harsh basic conditions and cannot be performed directly on peptides.[12] as a result, numerous approaches to label peptides with ^{18}F were developed, including bioconjugation with prosthetic groups like *N*-succinimidyl-4-[^{18}F]fluorobenzoate ([^{18}F]SFB) or *p*-nitrophenyl-2-[^{18}F]fluoropropionate ([^{18}F]NFP),[13] or more recent methodologies involving Al^{18}F chelation[14] or the “less conventional” use of organosilicon-based fluoride acceptor.[15] Among the recent chemoselective ^{18}F-labeling strategies involving indirect labeling by means of [^{18}F]-prosthetic groups, the popular alkyne-azide copper(I) catalyzed cycloaddition (CuAAC) “click” reaction, where the coupling of an azide and an alkyne leads to the formation of a triazole ring, appeared well suited for our purpose. It has been shown to be widely applicable and efficient for the labeling of peptides, mostly requiring a two-step synthetic approach. The success of this strategy and its wide range of application led to the development of a large variety of ^{18}F-labeled prosthetic groups as exemplified on Figure 1 and recently reviewed.[16,17] Thus, the one-step radiolabeling of suitable precursors followed

by cycloaddition of the resulting ^{18}F-bearing alkyne prosthetic groups with azido functionalized peptides of interest was shown to result in total RCYs of 20 – 75% (d. c.).[18–20] The corresponding radiosyntheses utilizing an ^{18}F-labeled azido prosthetic group and an alkyne functionalized peptide were shown to be equally efficient.[21–23]

With regards to the radiochemistry however, only a few of the common ^{18}F-labeled prosthetic groups like 1-(azidomethyl)-4-[^{18}F]-fluorobenzene[24] or 4-[^{18}F]fluoro-*N*-methyl-*N*-(prop-2-ynyl)-benzenesulfonamide,[20] are UV-detectable. A common disadvantage of [^{18}F]-fluoroalkynes or azides is also their high volatility, which can be technically challenging.[13, 18, 19, 21, 25] Finally, the preparation of [^{18}F]-glycosylazides or azidomethyl-[^{18}F]-benzenes for example involves more than one step and is therefore more laborious.[22] Besides these inherent difficulties of a prosthetic group radiosynthesis, to the best of our knowledge, only Hausner *et al.* have demonstrated an efficient ^{18}F-radiolabeling of peptides with a high molecular weight (MW > 2000 Da), commenting on the increasing challenge to label peptides with increasing complexity and size.[13] Ramenda *et al.* have reported the ^{18}F-radiolabeling of azide-functionalized Human Serum Albumin but noted that the introduction of azide residues into HSA and subsequent radiolabeling via click chemistry significantly altered the structural and functional integrity of HSA.[20] More recently, in an eloquent approach, Gill et al. have demonstrated the utility of maleimide functionalized alkyne in labeling antibodies with [^{18}F]-fluorine via a click approach.[26] However, the presence of cysteine and lysine residues in the pHLIP amino acid sequence makes this approach unrealistic in our case, as it is necessary to limit the number of derivatization sites to one in order to preserve the unique pHLIP properties. Therefore, it appears that further efficient ^{18}F-labeling procedures are necessary for the development of a successful and widely applicable [^{18}F]-pHLIP derivative.

Herein we report on the use of a novel ^{18}F-labeled prosthetic group for the efficient two-step "click" radiolabeling of azidohexanoic acid derivatized pHLIP involving a UV-detectable prosthetic group. The ultimate aim of this study was to evaluate the novel prosthetic group for its universal utilization in [^{18}F]-peptide chemistry. Therefore, the reaction conditions were investigated with two different peptides: D-WT-pHLIP (all amino acids have D configuration) and L-K-pHLIP (all amino acids have L configuration), which has the exact same sequence as WT-pHLIP but two aspartic acid residues have been replaced with lysines. These aspartic acid residues are present in the transmembrane part after insertion and are critical for pH dependent behavior. Therefore L-K-pHLIP lacks pH-dependent behavior and was used as a negative control in our study.[6, 27, 28] *In vitro* stability of the [^{18}F]-D-WT-pHLIP in both human and murine plasma was also examined. Finally, PET imaging and biodistribution studies were performed in order to determine the *in vivo* properties of the novel [^{18}F]-pHLIP conjugates in LNCaP and PC-3 tumor xenografts bearing mice.

MATERIALS and METHODS

General methods

All chemicals and solvents were purchased from Sigma-Aldrich, Anichem or Fluka and were used without further purification unless specifically stated otherwise. All peptide starting materials were purchased from C S Bio Co. (Menlo Park, CA, USA). Ultra-pure water was used in this work (>18 MΩcm^{-1} at 20 ºC, Milli-Q, Millipore, Billerica, MA, USA). All instruments were maintained and calibrated regularly according to quality control procedures as previously reported. Thin layer chromatography performed on pre-coated silica gel 60 F245 aluminium sheets suitable for UV detection of compounds was used for monitoring the reactions. Radioactivity measurements were performed with a Capintec CRC1243 Dose Calibrator (Capintec, Ramsay, NJ, USA). Precise quantification of low

radioactivity samples was achieved with a Perkin Elmer (Waltham, MA, USA) Automatic Wizard2 Gamma Counter. Nuclear magnetic resonance spectra were recorded on a Bruker AVIII 500.13 MHz spectrometer with an internal standard from solvent signals. Chemical shifts are given in parts per million (ppm) relative to tetramethylsilane (0.00 ppm). Values of the coupling constant, J, are given in hertz (Hz). The following abbreviations are used for the description of ^{1}H NMR and ^{13}C NMR spectra: singlet (s), doublet (d), doublet of doublets (dd), triplet (t), quartet (q). The chemical shifts of complex multiplets are given as the range of their occurrence. Low resolution mass spectra (LRMS) were recorded with a Waters Acquity UPLC with electrospray ionization SQ detector (ESI). High resolution mass spectra (HRMS) were recorded with a Waters LCT Premier system (ESI) and MALDI TOF analysis was performed on a Bruker Ultraflex TOF/TOF MALDI tandem TOF mass spectrometer. Quality control and purification of the final products in order to confirm the purity ≥ 95% of the radioactive intermediates and final products were achieved by analytical or semipreparative high performance liquid chromatography (HPLC). All HPLC experiments were performed on a Shimadzu HPLC system equipped with a Flow Count PIN diode radiodetector from BioScan, a DGU-20A degasser, two LC-20AB pumps, and SPD-M20A photodiode array detector and a SPD-M20A autosampler using reversed phase columns: (1) semipreparative: Luna 5 Uμ C18, 100 Å, 250 × 10 mm, (Phenomenex, Torrance, CA) (2) analytical: Luna 5 Uμ C18, 100 Å, 250 × 4.6 mm, (Phenomenex, Torrance, CA) (3) semipreparative: Nova-Pak 6 Uμ C18, 60 Å, 300 × 7.8 mm, (Waters, Milford, MA). Different gradient solvent systems were applied: (A) 20% – 80% MeCN in water in the presence of 0.1% trifluoroacetic acid (TFA) in 20 min with a flow of 5 mL/min; (B) 20% – 80% MeCN in water with 0.1% TFA in 20 min with a flow of 1.5 mL/min; (C) 5% – 40% EtOH in water in 5 min, 40% EtOH in water from 5–15 min with a flow rate of 3 mL/min.

Chemistry

Syntheses of cold reference compounds **2** to **5** are presented on Scheme 1.

2-((*Tert*-butyldimethylsilyl)ethynyl)-6-fluoropyridine (2)

To a degassed solution of *tert*-butyl(ethynyl)dimethylsilane (190 mg, 1.30 mmol) in triethylamine (Et_3N, 0.6 mL) and DMF (2 mL) was added CuI (50 mg, 0.26 mmol). To a second degassed solution of 2-bromo-6-fluoropyridine (200 mg, 1.10 mmol) in DMF (4 mL) was added $Pd(PPh_3)_4$ (15 mg, 0.013 mmol). Both mixtures were stirred for 5 min and then combined and allowed to react at RT for 24 h before saturated aqueous NH_4Cl (7 mL) was added. The resulting solution was then extracted with diethylether (Et_2O, 3 × 20 mL). The combined organic layers were washed with water (2 × 20 mL) and brine (20 mL) before drying over Na_2SO_4. Careful evaporation resulted in a brown oily residue. Purification by silica gel column chromatography utilizing pentane/Et_2O (95:5) gave **2** (105 mg, 40%) as a colorless oil that formed white crystals at 4 °C. R*f* = 0.8 (Pentane : ethyl acetate; 9:1). ^{1}H NMR (500 MHz, $CDCl_3$): δ 7.71 (q, *J* = 7.7 Hz, 1H), 7.33 (d, *J* = 6.5 Hz, 1H), 6.88 (dd, *J* =1.3, 2.5 Hz, 1H), 0.99 (s, 9H), 0.20 (s, 6H). ^{13}C NMR (500 MHz, $CDCl_3$): 162.9 (d, *J* = 241.2 Hz), 141.0 (d, *J* = 12.7 Hz), 125.0 (d, *J* = 3.9 Hz), 124.8 (d, *J* = 54.22 Hz), 109.6 (d, *J* = 36.9 Hz), 102.9, 95.0, 26.1, 16.7, 1.0. ^{19}F NMR (500 MHz, $CDCl_3$) : δ −65.17. MS *m/z* : 236.21 $(M + H)^+$.

2-Ethynyl-6-fluoropyridine (3)

To a solution of **2** (30 mg, 0.12 mmol) in dry tetrahydrofuran (THF, 2.5 mL) was added tetrabutylammonium fluoride (TBAF) trihydrate (120 mg, 0.38 mmol). After stirring the reaction mixture for one hour at RT, water (10 mL) was added. This mixture in water/THF (1:4) was used without further purification for the synthesis of the fluorinated reference

peptides. For analytical purposes, compound **3** was purified by semipreparative HPLC using the column 1 and the gradient solvent system A. The retention time of compound **3** was 11.2 min. Due to the volatility of the product and the small scale of the synthesis, concentration of the product was achieved using a C18 light cartridge (Waters) preconditioned with 5 mL of EtOH, followed by 5 mL of water. The combined fractions were diluted with water and passed over the cartridge. Pure product **3** was eluted with $CDCl_3$. ^{1}H NMR (500 MHz, $CDCl_3$): δ 7.76 (q, *J* = 7.8 Hz, 1H), 7.38 (d, *J* = 7.6 Hz, 1H), 6.94 (dd, *J* = 2.7, 2.9 Hz, 1H), 3.19 (s, 1H). ^{13}C NMR (500 MHz, $CDCl_3$): δ 162.9 (d, *J* = 237.8 Hz), 141.2 (d, *J* = 7.2 Hz), 125.4 (d, *J* = 96.37 Hz), 125.0 (d, *J* = 36.9 Hz), 110.2 (d, *J* = 36.8 Hz), 81.3, 78.3. ^{19}F NMR (500 MHz, $CDCl_3$): δ −65.30. MS *m/z* 121.89 $(M + H)^+$. HRMS calcd for C_7H_5NF, 122.0407; found, 122.0406.

6-(4-(6-Fluoropyridin-2-yl)-1*H*-1,2,3-triazol-1-yl)hexanoyl-D-WT-pHLIP (Fpyrtriazolo-D-WT-pHLIP, 4)

100 μL (0.01 mmol) of a freshly prepared solution of Cu(II) acetate (18 mg/mL) and 200 μL (0.02 mmol) of a fresh (+)-sodium L-ascorbate solution (20 mg/mL) in water were mixed in a sealed vial under argon. To the yellow mixture was added a solution of azidohexanoyl-D-WTpHLIP ($N_3(CH_2)_5$CONH-ACEQNPIYWARYADWLFTTPLLLLDLALLVDADEGTG-CO_2H) in EtOH (5 mg in 300 UL, 0.0012 mmol). Further addition of 2.7 μL of the solution of **3** (0.025 mmol) in water/THF (1:4) was followed by stirring of the reaction mixture at RT for 70 h before MeCN (3 mL) and water (3 mL) were added. The product was purified using semipreparative HPLC (column 1, solvent gradient system A): two conformational isomers (**4a**, **4b**) of Fpyrtriazolo-D-WTpHLIP were obtained with t_{R1} = 18.7 min and t_{R2} = 20.1 min, respectively. HPLC analysis indicated that the overall chemical purity of the compound **4** (**4a** + **4b**) is >98%. Calculated monoisotopic mass for Fpyrtriazolo-D-WTpHLIP ($C_{206}H_{301}FN_{48}O_{58}S$): 4426.18. **4a**: found, MS (MALDI) *m/z* = 4426.65, **4b**: found, MS (MALDI) *m/z* = 4426.56.

6-(4-(6-Fluoropyridin-2-yl)-1*H*-1,2,3-triazol-1-yl)hexanoyl-L-K-pHLIP (Fpyrtriazolo-L-K-pHLIP, 5)

This compound was prepared in an analogous way to compound **4**. The mixture containing the azidohexanoyl-L-K-pHLIP ($N_3(CH_2)_5$CONH-ACEQNPIYWARYAKWLFTTPLLLLKLALLVDADEGTG-CO_2H, 7.7 mg, 1.18 μmol) was stirred at RT for 48 h. Purification of the product was achieved by semipreparative HPLC on column 1 using the gradient solvent system A: t_R = 15.7 min; 99% purity. Calculated monoisotopic mass for peptide **5** ($C_{210}H_{315}FN_{50}O_{54}S$): 4452.31; found, MS (MALDI) *m/z* = 4452.724.

Radiochemistry

Radiosyntheses of [^{18}F]-3 to [^{18}F]-5 are presented on Scheme 2.

Radiosynthesis of [^{18}F]-3

[^{18}F]-fluoride (1480 – 2220 MBq) was obtained via the ^{18}O(p,n)^{18}F reaction of 11-MeV protons in an EBCO TR-19/9 cyclotron using enriched ^{18}O-water. QMA light cartridges (Waters) preconditioned with 0.5 M K_2CO_3 (5 mL) and water (5 mL) were used for trapping of $^{18}F^-$ from the aqueous solution. In order to elute $^{18}F^-$ from the cartridge into a sealed 5 mL reaction vial, 1 mL of Kryptofix K_{222} solution (Kryptofix K_{222}, 2.5 mg; K_2CO_3, 0.5 mg in MeCN/water (3:1)) was slowly passed through the cartridge. The solvents were evaporated at 110 ºC under vacuum in the presence of slight inflow of argon gas. After addition of MeCN (1 mL), azeotropic drying was achieved under vacuum and with a slight argon inflow. For the complete removal of water traces, the procedure was repeated twice. A

solution of the corresponding precursor **6** (Anichem), 1.5 – 2 mg in 200 μL of dry DMSO, was added to the Kryptofix complex and the reaction mixture was heated at 130 ºC for 10 min before 1 mL of water and 0.4 mL of MeCN were added (total injection volume 1.6 mL). Purification by semipreparative HPLC was carried out using the reversed phase column 3 with the gradient solvent system C: the product was eluted with the same retention time as the cold standard **3**: t_R = 9.2 min. Under the conditions used, the bromo precursor **6** has a retention time of 10.8 min. Identification of [^{18}F]-**3** was achieved by co-injection with the reference **3** on the reversed phase column 1 and the solvent system A: t_R = 10.2 min (Figure 2A).

Radiosynthesis of [^{18}F]-4

Stock solutions of copper (II) acetate (18 mg/mL) and (+)-sodium L-ascorbate (20 mg/mL), respectively, were freshly prepared. A v-shaped 4 mL HPLC vial (MT-IT^{TM}, Prominence, SHIMADZU) was equipped with a stir bar, sealed and set under argon before 30 μL of the Cu(II) acetate solution and 60 μL of the (+)-sodium L-ascorbate solution were mixed. The prosthetic group [^{18}F]-**3** (150 – 500 MBq) was directly collected from the HPLC into the prepared 4 mL HPLC vial (V = 1.2 – 1.6 mL). A solution of azidohexanoyl-D-WT-pHLIP ($N_3(CH_2)_5$CONH-ACEQNPIYWARYADWLFTTPLLLLDLALLVDADEGTG-CO_2H, 1 mg, 0.2 μmol) in EtOH (150 μL) was added and the mixture was heated at 70 °C for 5 – 10 min. After addition of MeCN (100 μL), purification of the product was achieved using semipreparative HPLC on reversed phase column 1 with solvent system A (total injection volume 1.5 – 2.0 mL). Two main radioactive peaks were eluted with the same retention time as the cold reference compounds **4a** and **4b** that are conformational isomers. HPLC analysis indicated that the overall radiochemical purity of the compound **4** (**4a** + **4b**) is >98%. The radiolabeled peptide could not be isolated from the peptide starting material resulting in lowered apparent specific activity. Only [^{18}F]-**4a**, obtained in MeCN/water (3:1, 0.1% TFA), was used for *in vivo* evaluation. After dilution with 7 mL of water, the solution was passed over a C18 light Sep Pak cartridge (Waters), preconditioned with 5 mL of EtOH followed by 5 mL of water. The cartridge was washed with further 3 mL of water in order to remove traces of MeCN and TFA and the trapped [^{18}F]-D-WT-pHLIP ([^{18}F]-**4a**) was eluted with 0.5 – 1 mL of EtOH. Identification of [^{18}F]-**4a** was achieved by comparison of the retention time with the cold reference compound **4** eluted with identical retention time under the same HPLC conditions but injecting only 50 μL of the collected solution for analysis. After evaporation of the solvent under vacuum and a slight argon inflow, which was completed within 6–8 minutes, the product was formulated in saline with 3% ethanol for injection.

Radiosynthesis of [^{18}F]-5

The radiosynthesis and purification were achieved in an analogous way to [^{18}F]-**4**. For the formulation of an injectable solution of [^{18}F]-**5**, a cartridge purification step was performed as described above. The product was eluted with 1.5 mL of acidified EtOH containing 0.02% 2N HCl and the solvent was removed under vacuum and a slight argon inflow. [^{18}F]-**5** was formulated in phosphate buffer for injection after addition of 50 μL of 0.1 N NaOH for neutralization. Identification of [^{18}F]-**5** was achieved by comparison of the retention time with the cold reference compound **5** eluted with identical retention time under the same HPLC conditions.

Determination of the lipophilicity of [^{18}F]-4 and [^{18}F]-5 ($logD_{pH7.4}$)

As described by Wilson *et al.*[29] for the shake flask method, phosphate buffer (pH 7.4) saturated octanol (500 μL) and octanol saturated phosphate buffer (500 μL) were added to a microcentrifuge tube (1.5 mL, Eppendorf). Following the addition of 10 μL of the

radiotracer solution (approximately 37 kBq), the samples were first vortexed and then shaken for 15 min. For phase separation, the samples were centrifuged at 2348 rcf for 5 min. 50 μL of each layer were withdrawn carefully from each phase and pipetted into microcentrifuge tubes (Eppendorf) for measurement of the distribution of the activity with a gamma-counter (Wizard^2, Perkin Elmer). The experiment was performed in quintuplicate.

In vitro stability test

For the determination of the *in vitro* stability of ^{18}F-labeled pHLIP analogues, 20 μL of the model peptide [^{18}F]-D-WT-pHLIP ([^{18}F]-**4**) in EtOH were added to both human and murine plasma (380 μL) and incubated at 37 °C. After 60 and 120 min, aliquots of 180 μL were removed and added to an equal amount of MeCN for precipitation of the present proteins. After 5 min of centrifugation (21130 rcf), 4 °C), the supernatant was analyzed under semipreparative HPLC conditions as described for the purification of the radiolabeled peptides.

Tumor cell culture

Human prostate cancer cell lines LNCaP and PC-3 from the American Tissue Culture Collection (ATCC, Manassas, VA, USA) were cultured in a 5% CO_2 atmosphere at 37 °C. LNCaP cells were cultured in RPMI 1640 medium containing 10% fetal calf serum (FCS), 2 mM L-glutamine, 1 mM sodium pyruvate, 4.5 g/L glucose, 1.5 g/L sodium bicarbonate and 100 U/mL of penicillin and streptomycin. PC-3 cell were cultured in F-12 Kaighn's medium containing 10% FCS, 2 mM L-glutamine, 1.5 g/L sodium bicarbonate and 100 U/mL of penicillin and streptomycin. Cells were trypsinized in the absence of magnesium or calcium ions using a cocktail of 0.25% trypsin and 0.53 mM EDTA in Hank's buffered salt solution.

LNCaP and PC-3 tumor xenografts

Male athymic mice (NCRNU-M, 20–25 g) were obtained from Taconic Farms, Inc (Hudson, NY, USA) and were kept in the MSKCC vivarium for one week before any experimental handling was performed. The animals were allowed free access to water and food and all animal care and experimental procedures were approved by the Institutional Animal Care and Use Committee (IACUC). LNCaP and PC-3 tumor xenografts were induced on the right and the left shoulder of each mouse, respectively, by subcutaneous injection of the corresponding cell suspension in Matrigel (BD, Collaborative Biomedical Products, Inc., Bedford, MA, USA) and media (1:1) containing $5.0 \times 10^6 – 10^7$cells (viability > 90%) per injection (200 μL). All procedures were carried out under anesthesia (1.5% isoflurane). Because of the slow rate of growth of the LNCaP tumors, these tumors were implanted 14 days prior to the PC-3 tumor implantation to have similarly sized tumors for the imaging and biodistribution studies. Palpable tumors of similar size developed after 4 to 5 weeks after the initial tumor xenograft induction.

Small-animal PET imaging studies

PET imaging studies were conducted on a microPET Focus 120 rodent scanner (Concorde Microsystems). Dual tumor bearing mice (n = 4) with LNCaP tumor (right shoulder, V = 100 – 200 mm^3) and PC-3 (left shoulder, V = 100 – 200 mm^3) were administered [^{18}F]-**4** [160–170 μCi (5.9 – 6.3 MBq)] in 200 μL formulated solution (3% EtOH in saline) and control peptide [^{18}F]-**5** [260 μCi (9.8 MBq)] in 200 μL formulated solution (Phosphate Buffered Saline) via tail vein injection. Approximately 3 min prior to the PET scan, mice were anesthetized by inhalation of 2% isoflurane (Baxter Healthcare, Deerfield, IL, USA)/ oxygen gas mixture and placed on the bed of the scanner while anesthesia was maintained using 1.5% isoflurane/gas mixture. PET data for each mouse were recorded via a 15-min

static acquisition 2 and 4h post injection (p. i.). For the static images a minimum of 20 million coincidence events were detected.

An energy window of 350–700 keV and a coincidence timing window of 6 ns were used. Data were sorted into two-dimensional histograms by Fourier re-binning, and transverse images were reconstructed by filtered back-projection into a 128×128×63 (0.72×0.72×1.3 mm) matrix. The images were normalized to correct for non-uniformity of response of the PET, dead-time count losses, positron branching ratio and physical decay to the time of injection, but no attenuation, scatter or partial-volume averaging correction was applied. The measured reconstructed spatial resolution for the Focus 120 is approximately 1.6 mm in full width at half maximum at the center of the field of view. The counting rates in the reconstructed images were converted to percent of injected dose per weight (%ID/g) by use of a system calibration factor derived from the imaging of a mouse-sized water-equivalent phantom containing ^{18}F. Images were evaluated by region-of-interest (ROI) analysis using ASIPro VM software (Concorde Microsystems).

Combined histological/autoradiographic analysis

After the completion of the last imaging session, vascular perfusion marker Hoechst 33342 (15 mg/kg in 0.2 mL of sterile saline) was administered via the tail vein catheter. Series of contiguous fresh-frozen tumor sections of 10 μm thickness were cut and exposed to a phosphor-imaging plate (Fujifilm BAS-MS2325, Fuji Photo Film, Japan) for an appropriate length of time at −20 °C. Digital images of radioactivity distribution at 50 μm resolution were obtained. The same sections were subsequently used for immunofluorescence imaging of Hoechst 33342, and finally stained with H&E. Autoradiographic and histological images were registered using Adobe Photoshop CS3 software.

Postmortem biodistribution studies

Dual tumor bearing mice (LNCaP and PC-3 tumors) were randomized before the experiment. Only mice with palpable tumors (V = 0.5 – 1.5 cm^3) were utilized. In order to investigate the biodistribution of radioactivity upon [^{18}F]-D-WT-pHLIP ([^{18}F]-**4**) injection, the tracer [~ 39 μCi (1.4 MBq), 15 nmol, 150 – 250 μL] was administered intravenously to the mice (n = 4 per time point, 16 – 24 g). Four mice were euthanized at 2 and 4 h post injection (p. i.), respectively. The blood was collected immediately followed by quick removal of the tumors. The lung, liver, heart, kidneys, spleen, bone, muscle, stomach, small intestines (SI), large intestines (LI) and testes were taken as well. The individual tumors and further organs were weighed and the radioactivity in each sample was measured in the gamma counter. Activity concentrations were calculated as percentage injected dose per tissue weight. (%ID/g wet tissue).

As a negative control, a formulated solution of [^{18}F]-**5** [55 μCi (2 MBq), 3.5 nmol)] was administered to a further group of dual tumor bearing mice (n = 4, 19 – 22 g). These mice were euthanized at 2 h p. i. and biodistribution performed as above.

RESULTS AND DISCUSSION

Recently, the CuAAC “click reaction” has attracted increasing interest for the ^{18}F-labeling of peptides, mainly because of the recent development of novel [^{18}F]-prosthetic groups and efficient protocols for this type of chemistry.[16, 17, 30] However, the feasibility of such methods for the synthesis of large [^{18}F]-peptides (MW > 2000 Da) has yet to be proven. Indeed, the preparation of an ^{18}F-labeled $\alpha_v\beta_6$ specific 20 amino acids peptide by Hausner *et al.* in 2008 is the only successful report,[13] which demonstrates the challenge of labeling large peptides efficiently without affecting their integrity.

We experienced numerous difficulties during our first attempts to synthesize ^{18}F-labeled WT-pHLIP via CuAAC using a previously described [^{18}F]fluoro-PEG-alkyne. Indeed, even though such a prosthetic group has been used successfully for the radiolabeling of RGD constructs,[18] no "click coupling" with azido-derivatized pHLIP analogues was observed in the standard CuAAC conditions that we used (Cu(II) acetate/(+)-sodium L-ascorbate in H_2O/CH_3CN 1:1). We were therefore interested in the development of a novel fluorinated prosthetic group and a corresponding synthetic procedure (Scheme 1), suitable for the radiolabeling of large peptides. We chose Fluoropyridinealkyne **3** because of the commercial availability of the corresponding bromo-precursor **6**, its UV-detectability, and the fact that 2-[^{18}F]fluoropyridines were shown to display high *in vivo* stability.[31] Moreover, the small size of **3** was expected to have a very limited impact on the pharmacokinetic of peptides as large as pHLIP.

Radiochemistry

[^{18}F]-**3** was prepared in one step by nucleophilic fluorination of the corresponding bromo precursor **6** (Scheme 2) using Kryptofix and K_2CO_3. Optimized conditions (DMSO, 10 min, 130 °C) led to [^{18}F]-**3** in RCYs of 27.5 ± 6.6% (n = 11) decay corrected (d. c.), with conversion rates between 70 and 90%. This high labeling efficacy was not translated into higher RCYs because a loss of radioactivity was systematically observed during the transfer to the HPLC, presumably due to the volatility of [^{18}F]-**3**. Although a distillation-based purification might allow for higher yields, like those obtained with volatile [^{18}F]fluoroalkynes prosthetic groups,[19] it would also introduce MeCN, which in our case was not favorable for the subsequent "click" reaction. Instead, technical improvements or pH adjustments could potentially minimize the effect of the pyridine alkyne volatility issue. Our HPLC purification has as principal advantage to afford [^{18}F]-**3** in high radiochemical purity (RCP > 98%, Figure 2A) in a mixture of ethanol and water, which appeared to be a perfectly suitable solvent system for the CuAAC with pHLIP. Indeed, full incorporation of [^{18}F]-**3** was achieved within 10 min at 70 °C as demonstrated by the HPLC chromatograms on Figure 2B and 2C, where no unreacted material [^{18}F]-**3** was detected.

The two peaks observed on Figure 2B are due to acidic HPLC conditions, which promotes the formation of two pH-dependent conformational isomers (**4a** and **4b**). When either of the peaks were collected separately and reinjected, we observed two peaks in HPLC indicating that these are same chemical species. This fact has also been confirmed by HPLC-MS. No dimerization of peptide (through cysteine-cysteine disulfide linkage) was observed. It is also interesting to note that conformational isomers were only observed in the case of WT-pHLIP (Figure 2B), which reflects the non acidity-dependent behavior of K-pHLIP (Figure 2C). Figure 2 also reveals that the radiolabeled peptides [^{18}F]-**4** and [^{18}F]-**5** could not be separated from the azido-derivatized starting materials. Consequently, the apparent specific activities were low (0.1 – 1 GBq/μmol), which should not question the use of [^{18}F]-pHLIP as an efficient PET tracer anyway. Indeed, given the mechanism of pHLIP insertion across the cell membrane, the number of insertion sites is theoretically unlimited wherever an acidic microenvironment is present,[7] as opposed to receptor based targeting systems.[32]

Considering the size and the complexity of the [^{18}F]-pHLIP analogues, the detailed radiochemical data obtained with [^{18}F]-**4** and [^{18}F]-**5** (Table 1) show the high efficacy of our novel strategy using [^{18}F]-**3**. Total RCYs of up to 20% could be achieved with respect to the starting amount of [^{18}F]-fluoride activity in a short synthesis time (≤ 85 min) and in one step, whereas several of the UV-detectable prosthetic groups that were used for peptide labeling were produced after multi-step radiosyntheses.[22, 23, 33] The total radiochemical yields also reflects that some radioactivity was lost during the transfers and on the HPLC, which leads to reduced overall yields. In our preparative HPLC conditions we never

observed any unreacted [^{18}F]-**3** or other byproducts in the reaction. Although better yields were reported with small-size peptides,[16] the CuAAC for was never achieved in such high yields with large peptides. By comparison, Hausner *et al.* radiolabeled a 20 amino acid peptide via "click" reaction in yields below 10%.[13] Finally, our novel ^{18}F-labeling protocol was performed with low amounts of copper, and a minimum of 1 mg peptide starting material was necessary to achieve complete incorporation of [^{18}F]-**3**, which is in line with previously reported ^{18}F-"click" reactions on larger peptides.[13]

For the characterization of the novel ^{18}F-labeled pHLIP analogues, a $logD_{pH7.4}$ determination was carried out (Table 1). [^{18}F]-**4a** and [^{18}F]-**4b** eluted from the HPLC system with different retention times and relative lipophilicity, exhibited the same $logD_{pH7.4}$ of −0.7 presumably due to isomerization and formation of the same equilibrium state at pH 7.4. [^{18}F]-**5** was eluted from the HPLC system with shorter retention time, and it accordingly displayed a $logD_{pH7.4}$ of −1.30 ± 0.03. It is well accepted that most of the [^{18}F]-prosthetic groups (Figure 1) lead to more lipophilic ^{18}F-labeled peptides, especially as the "click" approach involves the formation of a lipophilic triazole ring, often considered as a surrogate for the amide bond.[16,34] Although a similar effect is expected with the use of [^{18}F]-**3**, the small size of the prosthetic group and the triazole ring should only have a limited impact on the pharmacological properties of future investigated peptides.

The stability of the [^{18}F]-prosthetic group in the [^{18}F]-peptide construct is important in terms of clearance and metabolism. In particular, *in vivo* radio-defluorination is easily detectable because of the related bone uptake of radioactivity.[32] Therefore, [^{18}F]-**4a,** as a prominent pHLIP analogue was first subjected to an *in vitro* stability test in human and murine plasma at 37 °C. The tracer displayed a good stability: after 60 min, 80% and 100% of the parent tracer remained intact in human and murine plasma, respectively ; 65% and 85% were still present after 120 min. The degradation products were more hydrophilic and displayed retention times (t_R) suggesting potential peptide fragments. [^{18}F]-Fluoride is very hydrophilic and an elution from the HPLC column within the first 3 min is expected. However, no radioactive peaks were detected during the first 10 min. The fact that peptides derived from D-amino acids were shown to display higher *in vivo* stability,[35, 36] and the good *in vitro* stability of the D-WT-pHLIP analogue, [^{18}F]-**4a**, encouraged the *in vivo* evaluation of the novel peptide tracers.

PET imaging studies

In order to prove the ability of [^{18}F]-**4a** to target acidity, we chose two prostate carcinoma tumor models, LNCaP and PC-3. Indeed, as determined by magnetic resonance, Vavere *et al.* reported a significantly more acidic average pH_e for LNCaP tumors when compared with the PC-3 tumors.[9] Therefore, we were hopeful that this difference could be observed with PET following [^{18}F]-**4a** administration.

As a matter of fact, the LNCaP tumor could be clearly visualized at both time points (Figure 3) and exhibited a radioactivity accumulation of 8.3 ± 1.5 and 8.5 ± 1.3%ID/g at 2 and 4 h p.i., respectively. The PC-3 tumor showed lower radioactivity accumulation of 4.2 ± 0.4 to 5.4 ± 0.5%ID/g at 2 and 4 h p.i, respectively, and was poorly visualized. The lower uptake is a good indication for the successful application of the pHLIP principle for PET imaging of acidic tumors. Another indication for the specificity of the pHLIP was the lack of any tumor accumulation observed with the negative control peptide [^{18}F]-K-pHLIP (Figure 3).

The MR studies reported by Vavere *et al.* determined the total volume average pH_e in the tumors, but the heterogeneity of the tumor microenvironment suggests the formation of acidic and non-acidic areas in tumors. Accordingly, the PET images acquired after [^{18}F]-**4a** administration displayed a heterogeneous distribution of the tracer in the tumor since hot

spots within the LNCaP tumor could be visualized, indicating the specific enrichment of pHLIP analogues in acidic regions. Therefore, following PET imaging at 4h p. i., tumors were excised, sectioned and evaluated by digital autoradiography for ^{18}F-distribution. This distribution was subsequently compared to the distribution of the vascular perfusion marker Hoechst 33342 using the same section. A clear pattern of higher ^{18}F uptake in tumor regions lacking vascular perfusion was observed (Figure 4). Previous studies have shown that tumor regions with low vascular perfusion are associated with low pO2 and anaerobic glycolysis, resulting in lactate accumulation and reduced pH.[37] The accumulation of [^{18}F]-**4a** in tumor regions lacking vascular perfusion is consistent with the proposed mechanism of pHLIP accumulation, and corroborates the specificity underlying the heterogeneous tumor distribution observed in the PET imaging.

For both tracers, the PET images exhibited the highest radioactivity concentrations in the liver indicating that [^{18}F]-**4a** and [^{18}F]-**5** are mainly excreted via the hepatobiliary system. Little radioactivity accumulation was detected in the bone in all PET imaging studies performed with the [^{18}F]-pHLIP radiotracer that were radiolabeled using our novel [^{18}F]-labeling protocol, pointing to a high *in vivo* stability of the [^{18}F]-prosthetic groups. The high activity observed in the liver might preclude the use of the tracer for imaging tumors near the liver.

Biodistribution

Biodistribution studies were performed with [^{18}F]-**4a** and [^{18}F]-**5** in mice with dual PC-3 (left) and LNCaP (right) tumors on the shoulders. Based on our preliminary imaging studies we chose the 2 and 4 h time points for the biodistribution study. Figure 5 shows the distribution of radioactivity in mice of [^{18}F]-**4a** at 2 and 4 h p.i. and of [^{18}F]-**5** at 2 h. For [^{18}F]-**4a**, the highest accumulation of radioactivity in LNCaP tumors was observed at 4 h p.i.. The uptake in PC-3 tumors was much lower at both time points. At 4 h p.i. LNCaP tumors had uptake of 8.0 ± 0.7 %ID/g as compared to PC-3 tumors which had uptake 5.3 ± 0.7 %ID/g. These results are in line with our earlier publication[9] with [^{64}Cu]-DOTA-pHLIP (all L amino acids) and with PET imaging studies.

The highest accumulation of radioactivity at both time points was detected in the liver (32.5 ± 4.3%ID/g and 34.9 ± 5.8%ID/g at 2 and 4 h p. i., respectively), followed by the kidneys. As expected with large hydrophobic peptides the blood clearance was slow. [^{64}Cu]-pHLIP shows highest accumulation in LNCaP tumors at 1 h p. i. (4.5 ± 1.7%ID/g) and highest tumor to blood ratio at 24 h p.i.[9].

The tumor-to-tissue ratios for [^{18}F]-**4a** and [^{18}F]-**5** are shown in Table 2. The tumor (LNCaP)-to-liver and the tumor (LNCaP)-to-kidney ratios are 0.2 and 0.3, respectively, both at 2 and 4 h. From our limited biodistribution studies it is difficult to differentiate between excretory and metabolic factors contributing to these high values. As shown in table 2, the negative control peptide [^{18}F]-**5** exhibits similar ratios in liver and kidney. It can be hypothesized that the activity in these organs is due to excretion rather than metabolism. The tumor–to-muscle ratio of 4.5 measured at 2 h p. i. with [^{18}F]-**4a** in comparison to 0.4 with [^{18}F]-**5**, demonstrates we are specifically targeting the tumor with [^{18}F]-**4a** and is not a result of non-specific accumulation. The tumor-to-muscle ratio is even higher at 4 h p. i. with a value of 5.7. These studies clearly demonstrate that this click approach with prosthetic group **3** has no negative impact on the biological properties of pHLIP. Additionally, higher %ID/g values in LNCaP tumors as compared to the PC-3 tumor indicate that the accumulation of the tracer reflects acidity of the tissue.

[^{18}F]-pyridines labeled at ortho-position to the nitrogen have been reported to be stable against in vivo defluorination.[31] However, we observe some bone uptake with [^{18}F]-**5** (1.31

± 0.63 %ID/g) and [^{18}F]-**4a** (4.14 ± 1.12 %ID/g) 2h p. i.. In comparison, [^{18}F]-Fluoropentyne based prosthetic group shows very minimal bone uptake (0.39 %ID/g at 1h p.i.). In our case, it is unclear whether the uptake is result of defluorination or specific accumulation, because the two peptides radiolabeled wth same prosthetic group show different bone uptake values.

CONCLUSION

We have extended the use of the CuAAC "click chemistry" with the development of 2-ethynyl-6-[^{18}F]fluoro-pyridine as a new prosthetic group suitable for the ^{18}F-labeling of large peptides. This approach should be widely applicable and was shown to be efficient for the radiolabeling of pHLIP analogues with a molecular weight over 4000 Da. Two ^{18}F-labeled analogues were injected in mice in order to acquire the first *in vivo* [^{18}F]-pHLIP data. The WT-pHLIP construct showed good *in vitro* stability and only mild *in vivo* defluorination was observed in both cases. A milestone in the development of a ^{18}F-labeled pHLIP tumor imaging agent was achieved, as the use of [^{18}F]-**3** will allow for the fast production and evaluation of second generation pHLIP analogues, designed for higher accumulation in the tumors and faster clearance from non-target tissues.

Acknowledgments

Grant Support: Funded in part by the NIH/NCI R01CA138468 (JSL) and the Office of Science (BER) - US Department of Energy (Award DE-SC0002456; JSL). Technical services provided by the MSKCC Small-Animal Imaging Core Facility were supported in part by NIH grants R24-CA83084 and P30-CA08748.

Funded in part by the NIH/NCI R01CA138468 (JSL) and the Office of Science (BER) - US Department of Energy (Award DE-SC0002456; JSL). Technical services provided by the MSKCC Small-Animal Imaging Core Facility were supported in part by NIH grants R24-CA83084 and P30-CA08748. Special thanks to Valerie Longo, Vadim Divilov, Kuntalkumar Sevak and Nicholas Ramos for technical support, Calvin Lom and Howard Sheh from the MSKCC Radiochemistry-Cyclotron Core and George Sukenick from the MSKCC Nuclear Magnetic Resonance (Analytical).

References

1. Bild AH, Potti A, Nevins JR. Linking oncogenic pathways with therapeutic opportunities. Nat Rev Cancer. 2006; 6(9):735–741. [PubMed: 16915294]
2. Gillies RJ. Causes and consequences of hypoxia and acidity in tumors. Novartis Foundation symposium. Trends Mol Med. 2001; 7(2):47–49. [PubMed: 11330256]
3. Cairns R, Papandreou I, Denko N. Overcoming physiologic barriers to cancer treatment by molecularly targeting the tumor microenvironment. Molecular cancer research : MCR. 2006; 4(2): 61–70. [PubMed: 16513837]
4. Sakamoto S, Ryan AJ, Kyprianou N. Targeting vasculature in urologic tumors: mechanistic and therapeutic significance. J Cell Biochem. 2008; 103(3):691–708. [PubMed: 17668426]
5. Hunt JF, Rath P, Rothschild KJ, Engelman DM. Spontaneous, pH-dependent membrane insertion of a transbilayer alpha-helix. Biochemistry. 1997; 36(49):15177–15192. [PubMed: 9398245]
6. Reshetnyak YK, Andreev OA, Lehnert U, Engelman DM. Translocation of molecules into cells by pH-dependent insertion of a transmembrane helix. Proc Nat Acad Sci USA. 2006; 103(17):6460–6465. [PubMed: 16608910]
7. Andreev OA, Dupuy AD, Segala M, Sandugu S, Serra DA, Chichester CO, Engelman DM, Reshetnyak YK. Mechanism and uses of a membrane peptide that targets tumors and other acidic tissues in vivo. Proc Nat Acad Sci USA. 2007; 104(19):7893–7898. [PubMed: 17483464]
8. Reshetnyak YK, Yao L, Zheng S, Kuznetsov S, Engelman DM, Andreev OA. Measuring tumor aggressiveness and targeting metastatic lesions with fluorescent pHLIP. Mol Imaging Biol. 2011; 13(6):1146–1156. [PubMed: 21181501]

9. Vavere AL, Biddlecombe GB, Spees WM, Garbow JR, Wijesinghe D, Andreev OA, Engelman DM, Reshetnyak YK, Lewis JS. A novel technology for the imaging of acidic prostate tumors by positron emission tomography. Cancer Res. 2009; 69(10):4510–4516. [PubMed: 19417132]
10. Ametamey SM, Honer M, Schubiger PA. Molecular imaging with PET. Chem Rev. 2008; 108(5): 1501–1516. [PubMed: 18426240]
11. Okarvi SM. Recent progress in fluorine-18 labelled peptide radiopharmaceuticals. European J Nucl Med. 2001; 28(7):929–938. [PubMed: 11504093]
12. Olberg DE, Hjelstuen OK. Labeling Strategies of Peptides with ^{18}F for Positron Emission Tomography. Curr Top Med Chem. 2010; 10(16):1669–1679. [PubMed: 20583991]
13. Hausner SH, Marik J, Gagnon MKJ, Sutcliffe JL. In Vivo Positron Emission Tomography (PET) Imaging with an αvβ6 Specific Peptide Radiolabeled using ^{18}F-"Click" Chemistry: Evaluation and Comparison with the Corresponding 4-[^{18}F]Fluorobenzoyl- and 2-[^{18}F]Fluoropropionyl-Peptides. J Med Chem. 2008; 51(19):5901–5904. [PubMed: 18785727]
14. McBride WJ, D'Souza CA, Sharkey RM, Karacay H, Rossi EA, Chang CH, Goldenberg DM. Improved ^{18}F Labeling of Peptides with a Fluoride-Aluminum-Chelate Complex. Bioconjugate Chem. 2010; 21(7):1331–1340.
15. Schirrmacher R, Bradtmoller G, Schirrmacher E, Thews O, Tillmanns J, Siessmeier T, Buchholz HG, Bartenstein P, Waengler B, Niemeyer CM, Jurkschat K. F-18-labeling of peptides by means of an organosilicon-based fluoride acceptor. Angew Chem Int Ed. 2006; 45(36):6047–6050.
16. Glaser M, Robins EG. 'Click labelling' in PET radiochemistry. J Labelled Compd Radiopharm. 2009; 52(9–10):407–414.
17. Mamat C, Ramenda T, Wuest FR. Recent Applications of Click Chemistry for the Synthesis of Radiotracers for Molecular Imaging. Mini-Rev Org Chem. 2009; 6(1):21–34.
18. Li Z-B, Wu Z, Chen K, Chin FT, Chen X. Click Chemistry for ^{18}F-Labeling of RGD Peptides and microPET Imaging of Tumor Integrin αvβ3 Expression. Bioconjugate Chem. 2007; 18(6):1987–1994.
19. Marik J, Sutcliffe JL. Click for PET: rapid preparation of [^{18}F]fluoropeptides using CuI catalyzed 1,3-dipolar cycloaddition. Tetrahedron Lett. 2006; 47(37):6681–6684.
20. Ramenda T, Kniess T, Bergmann R, Steinbach J, Wuest F. Radiolabelling of proteins with fluorine-18 via click chemistry. Chem Commun (Camb). 2009; 48:7521–7523. [PubMed: 20024266]
21. Glaser M, Årstad E. "Click Labeling" with 2-[^{18}F]Fluoroethylazide for Positron Emission Tomography. Bioconjugate Chem. 2007; 18(3):989–993.
22. Maschauer S, Einsiedel J, Haubner R, Hocke C, Ocker M, Hübner H, Kuwert T, Gmeiner P, Prante O. Labeling and Glycosylation of Peptides Using Click Chemistry: A General Approach to ^{18}F-Glycopeptides as Effective Imaging Probes for Positron Emission Tomography. Angew Chem Int Ed. 2010; 49(5):976–979.
23. Thonon D, Kech Cc, Paris Jrm, Lemaire C, Luxen A. New Strategy for the Preparation of Clickable Peptides and Labeling with 1-(Azidomethyl)-4-[^{18}F]-fluorobenzene for PET. Bioconjugate Chem. 2009; 20(4):817–823.
24. Thonon D, Paris J, Kech C, Lemaire C, Luxen A. Peptide Click Labeling with 1-(Azidomethyl)-4-[^{18}F]-Fluorobenzene and Solid Phase Synthesis of Reference Compounds. J Labelled Compd Radiopharm. 2009; 52:S26–S26.
25. Iddon L, Leyton J, Indrevoll B, Glaser M, Robins EG, George AJT, Cuthbertson A, Luthra SK, Aboagye EO. Synthesis and in vitro evaluation of [^{18}F]fluoroethyl triazole labelled [Tyr3]octreotate analogues using click chemistry. Bioorg Med Chem Lett. 2011; 21(10):3122–3127. [PubMed: 21458258]
26. Gill HS, Tinianow JN, Ogasawara A, Flores JE, Vanderbilt AN, Raab H, Scheer JM, Vandlen R, Williams SP, Marik J. A modular platform for the rapid site-specific radiolabeling of proteins with ^{18}F exemplified by quantitative positron emission tomography of human epidermal growth factor receptor 2. J Med Chem. 2009; 52(19):5816–5825. [PubMed: 19736996]
27. Reshetnyak YK, Andreev OA, Segala M, Markin VS, Engelman DM. Energetics of peptide (pHLIP) binding to and folding across a lipid bilayer membrane. Proc Nat Acad Sci USA. 2008; 105(40):15340–15345. [PubMed: 18829441]

28. Reshetnyak YK, Segala M, Andreev OA, Engelman DM. A monomeric membrane peptide that lives in three worlds: In solution, attached to, and inserted across lipid bilayers. Biophys J. 2007; 93(7):2363–2372. [PubMed: 17557792]
29. Wilson AA, Jin L, Garcia A, DaSilva JN, Houle S. An admonition when measuring the lipophilicity of radiotracers using counting techniques. Appl Radiat Isot. 2001; 54(2):203–208. [PubMed: 11200881]
30. Schirrmacher R, Wangler C, Schirrmacher E. Recent Developments and Trends in ^{18}F-Radiochemistry: Syntheses and Applications. Mini-Rev Org Chem. 2007; 4(4):317–329.
31. Dolle F. [^{18}F]fluoropyridines: From conventional radiotracers to the labeling of macromolecules such as proteins and oligonucleotides. Ernst Schering Research Foundation workshop. 2007; 62:113–157. [PubMed: 17172154]
32. Burns HD, Hamill TG, Eng W, Francis B, Fioravanti C, Gibson RE. Positron emission tomography neuroreceptor imaging as a tool in drug discovery, research and development. Curr Opin Chem Biol. 1999; 3(4):388–394. [PubMed: 10419855]
33. Ramenda T, Bergmann R, Wuest F. Synthesis of F-18-labeled neurotensin(8–13) via copper-mediated 1,3-dipolar [3+2] cycloaddition reaction. Lett Drug Des Discov. 2007; 4(4):279–285.
34. Demko ZP, Sharpless KB. A click chemistry approach to tetrazoles by Huisgen 1,3-dipolar cycloaddition: Synthesis of 5-sulfonyl tetrazoles from azides and sulfonyl cyanides. Angew Chem Int Ed. 2002; 41(12):2110–2113.
35. Miller SM, Simon RJ, Ng S, Zuckermann RN, Kerr JM, Moos WH. Comparison of the Proteolytic Susceptibilities of Homologous L-Amino-Acid, D-AminoAcid, and *N*-Substituted Glycine Peptide and Peptoid Oligomers. Drug Dev Res. 1995; 35(1):20–32.
36. Wade D, Boman A, Wahlin B, Drain CM, Andreu D, Boman HG, Merrifield RB. All-D Amino Acid-Containing Channel-Forming Antibiotic Peptides. Proc Nat Acad Sci USA. 1990; 87(12): 4761–4765. [PubMed: 1693777]
37. Yaromina A, Quennet V, Zips D, Meyer S, Shakirin G, Walenta S, Mueller-Klieser W, Baumann M. Co-localisation of hypoxia and perfusion markers with parameters of glucose metabolism in human squamous cell carcinoma (hSCC) xenografts. Int J Radiat Biol. 2009; 85(11):972–98. [PubMed: 19895274]

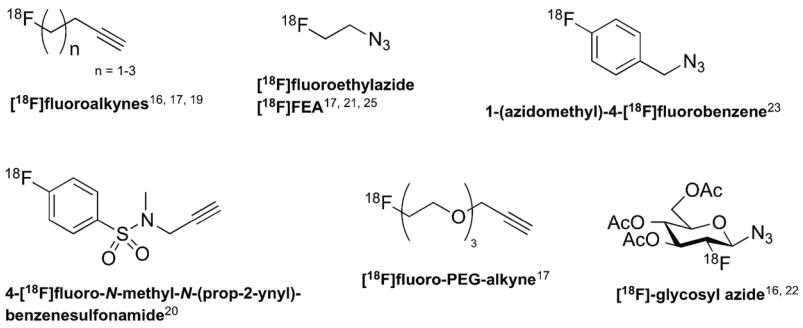

Figure 1.
Examples of [^{18}F]-labeled prosthetic groups for the CuAAC “click” reaction with functionalized peptides and proteins.

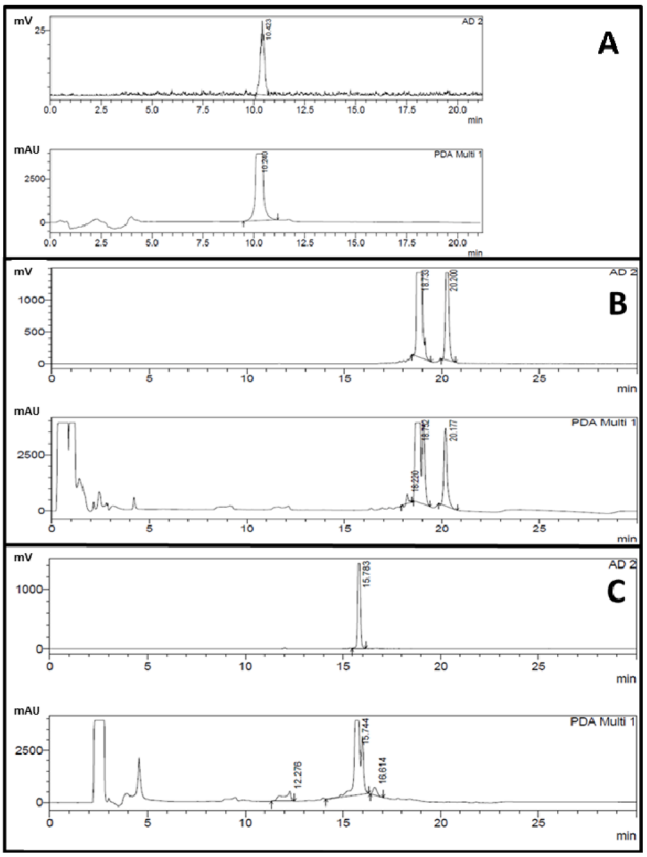

Figure 2.

HPLC chromatograms with radio and UV-traces (UV traces were recorded at 254 nm and retention times are given with respect to the radiotrace): (A) co-injection of compound **3** and [^{18}F]-**3** with t_R = 10.4 min on column 1; (B) purification of [^{18}F]-**4a** and −**4b** after 5 min at 70 °C with t_R = 18.7 min and t_R = 20.2 min, respectively; (C) purification of [^{18}F]-**5** after 5 min reaction at 70 °C (t_R = 15.8 min). HPLC chromatograms were recorded utilizing column 1 applying elution conditions A.

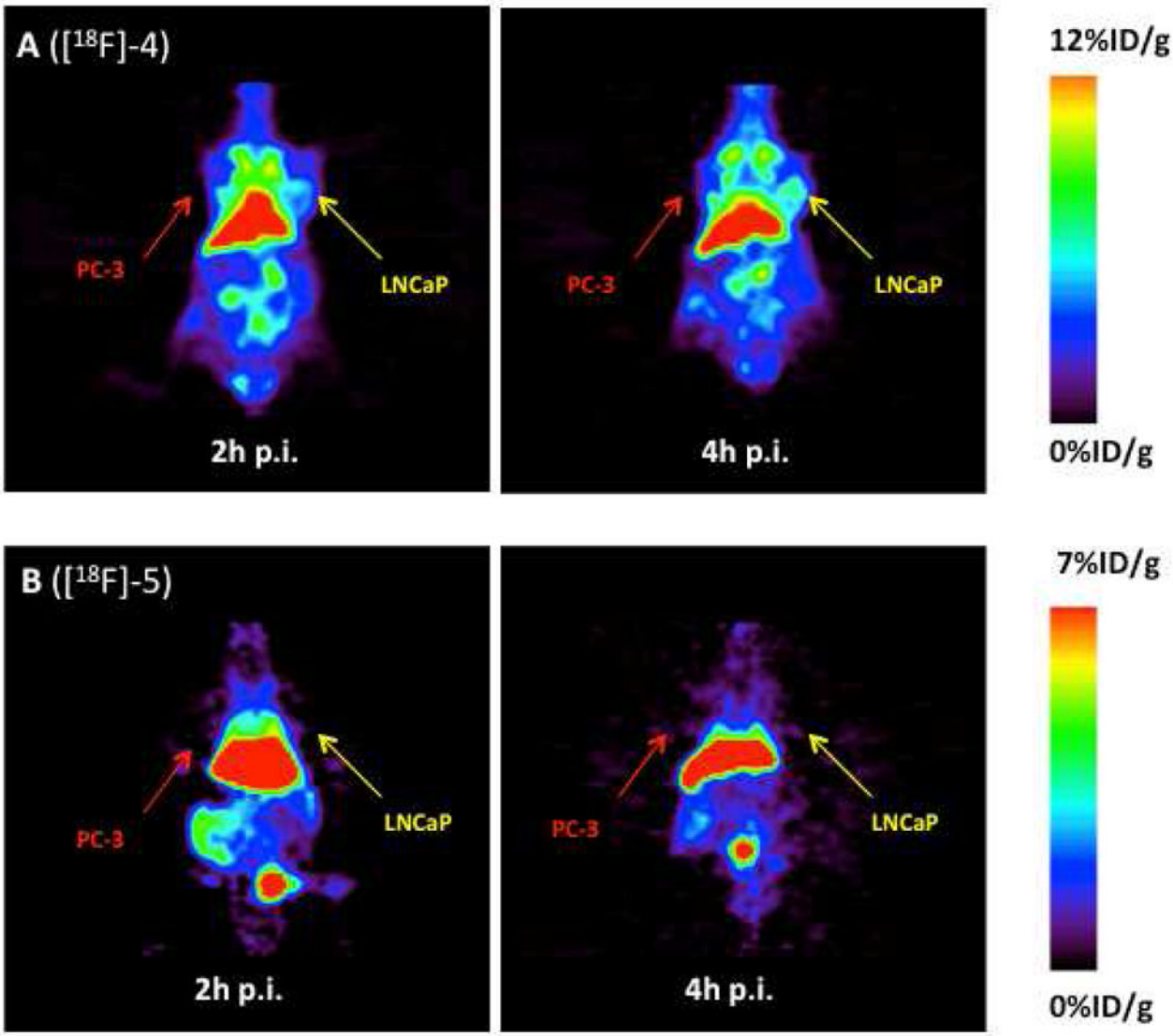

Figure 3.
Representative coronal PET images of mice bearing LNCaP (Right) and PC-3 (Left) tumors injected with [^{18}F]-**4** (A) and [^{18}F]-**5** (B).

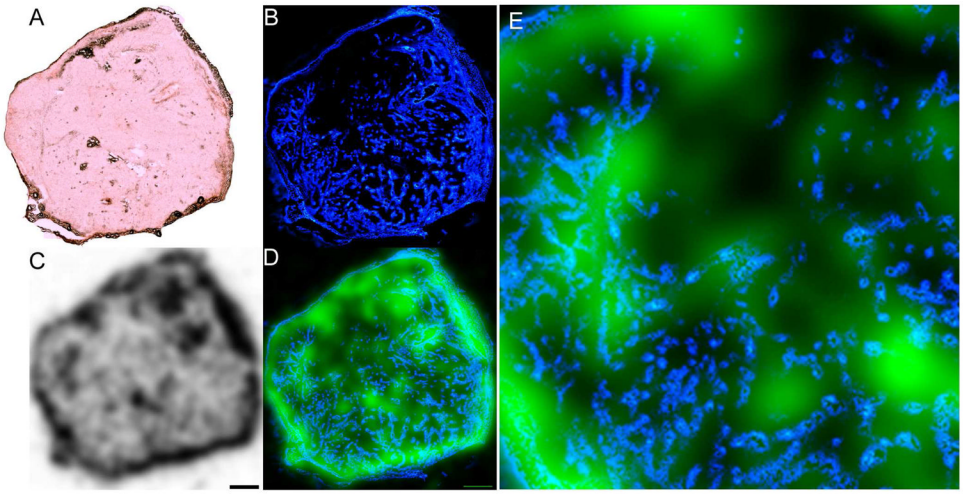

Figure 4.

Combined histological/autoradiographic analysis obtained after [^{18}F]-**4** injection (4h p. i.). Data from a single 10 μm frozen section obtained from a LNCaP tumor. H&E staining (panel A), the vascular perfusion marker Hoechst 33342 (blue, panel B) and autoradiograph of radioactivity distribution (panel C) are shown. Panel D shows co-registration of autoradiograph (pseudo-color green) overlaid with Hoechst 33342 (blue). Panel E contains a high-magnification region from the image shown in Panel D. Scale bar = 1mm.

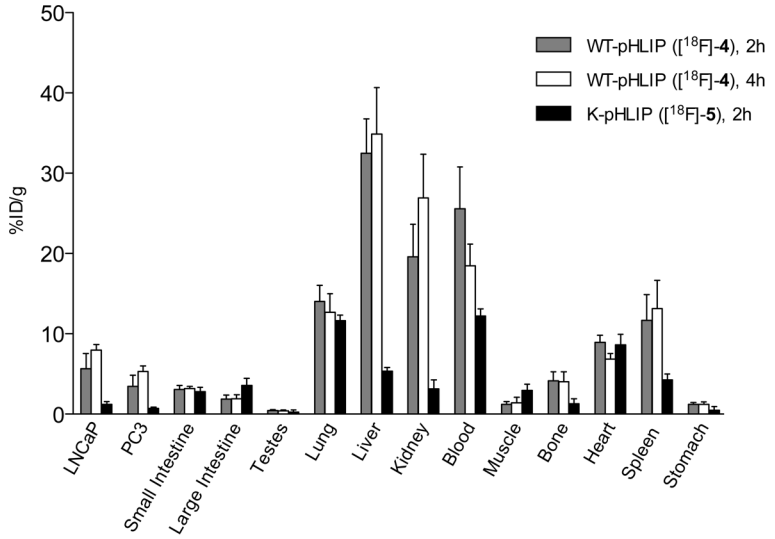

Figure 5.
Biodistribution of [^{18}F]-**4** and [^{18}F]-**5** at 2 and 4 h p. i. with uptake values expressed as %ID/g.

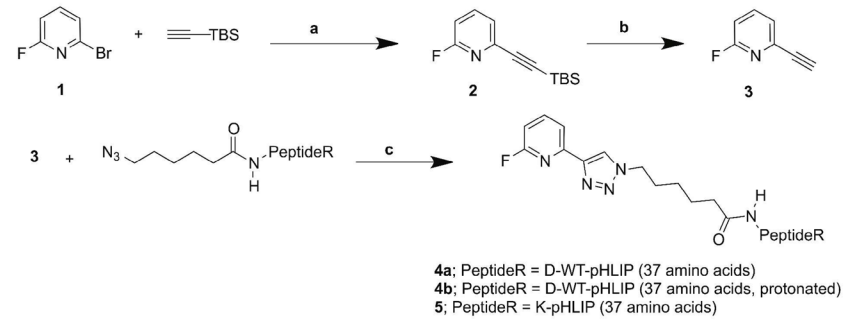

Reagents and conditions: (a) $Pd(PPh_3)_4$, CuI, Et_3N, DMF, RT, 24 h; (b) THF, TBAF, 1 h, RT; (c) H_2O, ACN, EtOH, Cu-acetate x 5 H_2O, sodium L-ascorbate, 48-70 h, RT.

Scheme 1.

Synthetic route yielding the non-radiolabeled reference compounds **3** to **5**.

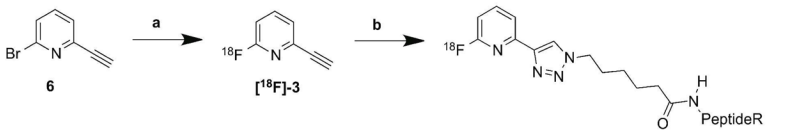

[18F]-4; PeptideR = D-WT-pHLIP (37 amino acids)
[18F]-5; PeptideR = K-pHLIP (37 amino acids)

Reagents and conditions: (a) K[18F]F-Kryptofix 222, DMSO, 130 °C, 10 min; (b) H_2O, EtOH, Cu-acetate x 5 H_2O, sodium L-ascorbate, azidohexanoic acid derivatised peptide, 70 - 80 °C, 5 - 10 min.

Scheme 2.
Radiosynthesis yielding radiolabeled products [^{18}F]-**3** to [^{18}F]-**5**.

Table 1

Analytical data determined for radiolabeled peptides [^{18}F]-**4a**, [^{18}F]-**4b** (n = 4) and [^{18}F]-**5** (n = 3) after semipreparative HPLC purification.

	RCP [%]	Total RCY [%]	Specific activity (EOS) [GBq/μmol]	Total preparation time [min]	$logD_{pH7.4}$
[^{18}F]-D-WT-pHLIP ([^{18}F]-**4a**)	≥ 95	13.6 ± 6.0	0.1 – 1.0	85	− 0.70 ± 0.04
[^{18}F]-D-WT-pHLIP ([^{18}F]-**4b**)	---		---		− 0.70 ± 0.20
[^{18}F]-L-K-pHLIP ([^{18}F]-**5**)	≥ 98	5 – 13	0.1 – 0.8		− 1.30 ± 0.03

Table 2

LNCaP tumor-to-tissue ratios determined upon biodistribution studies with the tracers administered to tumor bearing mice.

Tumor to Tissue ratio	[^{18}F]-4 2 h p. i.	[^{18}F]-4 4 h p. i.	[^{18}F]-5 2 h p. i.
Tumor/blood	0.2	0.4	0.1
Tumor/muscle	4.5	5.7	0.4
Tumor/liver	0.2	0.2	0.2
Tumor/kidney	0.3	0.3	0.4